Brostrom, C. O., Huang, Y. C., Breckenridge, B. M., & Wolff, D. J. (1975) *Proc. Natl. Acad. Sci. U.S.A. 72*, 64.
Brostrom, C. O., Brostrom, M. A., & Wolff, D. J. (1977) *J. Biol. Chem. 252*, 5677.
Cheung, W. Y., Bradham, L. S., Lynch, T. J., Lin, Y. M., & Tallant, E. A. (1975) *Biochem. Biophys. Res. Commun. 66*, 1055.
Dedman, J. R., Potter, J. D., Jackson, R. L., Johnson, J. D., & Means, A. R. (1977) *J. Biol. Chem. 252*, 8415.
Hanksi, E., Sevilla, N., & Levitzki, A. (1977) *Eur. J. Biochem. 76*, 513.
Howlett, A. C., & Gilman, A. G. (1980) *J. Biol. Chem. 255*, 2861.
Howlett, A. C., Sternweis, P. C., Macik, B. A., Van Arsdale, P. M., & Gilman, A. G. (1979) *J. Biol. Chem. 254*, 2287.
LaPorte, D. C., Toscano, W. A., & Storm, D. R. (1979) *Biochemistry 18*, 2820.
LeDonne, N. C., & Coffee, C. J. (1979) *Fed. Proc., Fed. Am. Soc. Exp. Biol. 38*, 317.
Limbird, L. E., Hickey, A. R., & Lefkowitz, R. J. (1979) *J. Biol. Chem. 254*, 2677.
Neer, E. J., & Salter, R. S. (1981) *J. Biol. Chem. 256*, 5497.
Northup, J. K., Sternweis, P. C., Smigel, M. D., Schleifer, L. S., Ross, E. M., & Gilman, A. G. (1980) *Proc. Natl. Acad. Sci. U.S.A. 77*, 6516.
Northup, J. K., Smigel, M. D., & Gilman, A. G. (1982) *J. Biol. Chem. 257*, 11416.
Peterson, G. L. (1977) *Anal. Biochem. 83*, 346.
Ross, E. M., & Gilman, A. G. (1980) *Annu. Rev. Biochem. 49*, 533.
Salomon, Y., Londos, D., & Rodbell, M. (1974) *Anal. Biochem. 58*, 541.
Schleifer, L. S., Kahn, R. A., Hanski, E., Northup, J. K., Sternweis, P. C., & Gilman, A. G. (1982) *J. Biol. Chem. 257*, 20.
Sternweis, P. C., Northup, J. K., Smigel, M. D., & Gilman, A. G. (1981) *J. Biol. Chem. 256*, 11517.
Valverde, I., Vandermeers, A., Anjaneyula, R., & Malaisse, W. J. (1979) *Science (Washington, D.C.) 206*, 225.
Westcott, K. R., LaPorte, D. C., & Storm, D. R. (1979) *Proc. Natl. Acad. Sci. U.S.A. 76*, 204.

Epidermal Growth Factor from the Mouse. Physical Evidence for a Tiered β-Sheet Domain: Two-Dimensional NMR Correlated Spectroscopy and Nuclear Overhauser Experiments on Backbone Amide Protons†

K. H. Mayo*

Department of Chemistry, Yale University, New Haven, Connecticut 06511, and Department of Chemistry, Temple University, Philadelphia, Pennsylvania 19122

Received May 7, 1984; Revised Manuscript Received December 27, 1984

ABSTRACT: When H_2O-exchanged, lyophilized mouse epidermal growth factor (mEGF) is dissolved in deuterium oxide at low pH (i.e., below ~6.0), 13 well-resolved, amide proton resonances are observed in the downfield region of an NMR spectrum (500 MHz). Under the conditions of these experiments, the lifetimes of these amide protons in exchange for deuterons of the deuterium oxide solvent suggest that these amide protons are hydrogen-bonded, backbone amide protons. Several of these amide proton resonances show splittings (i.e., $J_{NH\alpha\text{-}CH}$) of approximately 8–10 Hz, indicating that their associated amide protons are in some type of β-structure. Selective nuclear Overhauser effect (NOE) experiments performed on all amide proton resonances strongly suggest that all 13 of these backbone amide protons are part of a single-tiered β-sheet structural domain in mEGF. Correlation of 2D NMR correlated spectroscopy data, identifying scaler coupled protons, with NOE data, identifying protons close to the irradiated amide protons, allows tentative assignment of some resonances in the NOE difference spectra to specific amino acid residues. These data allow a partial structural model of the tiered β-sheet domain in mEGF to be postulated.

The protein hormone, mouse epidermal growth factor (mEGF),[1] stimulates the growth and differentiation of various epidermal and epithelial tissues (Cohen, 1962, 1965; Cohen & Elliott, 1963; Turkington, 1969; Savage & Cohen, 1973). On a cellular level, mEGF works directly on skin cells by binding to a transmembrane receptor molecule and becoming internalized in the cell by endocytosis (McKanna et al., 1979; Carpenter & Cohen, 1976). Binding of mEGF to the receptor molecule in the presence of ATP also generates an enhanced phosphorylation of a number of membrane proteins; the formation of this mEGF–receptor complex (Hollenberg & Cuatrecasas, 1973; Carpenter et al., 1975) most likely activates a protein kinase that is one part of the mEGF receptor polypeptide chain (Buhrow et al., 1982, 1983). Physiological

† This work was supported by a grant from the National Institutes of Health (GM-34662) and by a generous gift from the Glenmede Trust Fund and benefited from NMR facilities made available to Yale University through Grant CHE-7916210 from the National Science Foundation.

* Address correspondence to the author at the Department of Chemistry, Temple University.

[1] Abbreviations: mEGF, mouse epidermal growth factor; DSS, sodium 4,4-dimethyl-4-silapentanesulfonate; NOE, nuclear Overhauser effect; FID, free-induction decay; 2D NMR COSY, two-dimensional NMR correlated spectroscopy; CIDNP, chemically induced dynamic nuclear polarization.

0006-2960/85/0424-3783$01.50/0

effects of mEGF include increased uptake of salts and glucose, increased protein, RNA, and DNA synthesis, and cell division. Several reviews on the chemistry and biological actions of mEGF are available (Cohen & Taylor, 1974; Cohen & Savage, 1974; Cohen et al., 1975; Carpenter & Cohen, 1979).

Many studies of structure–function relationships of a variety of polypeptide hormones have indicated that the biological activity of these molecules is stringently dependent on a precise chemical and physical structure. This statement has, therefore, stimulated a great deal of interest in an elucidation of the three-dimensional structure of mouse epidermal growth factor. The primary structure of mEGF consists of a single polypeptide chain of 53 amino acid residues (6045 daltons) and contains three disulfide bonds (Taylor et al., 1972). Although the sequence of mEGF has been known for some time (Savage et al., 1973), attempts to crystallize the protein have been unsuccessful, and therefore, no X-ray crystallographic structure exists. The predictive Chou–Fasman secondary structural algorithm (Chou & Fasman, 1974a,b, 1978a,b) has been applied to mEGF (Holladay et al., 1976). The following regions of ordered secondary structure are predicted: two sections of β-structure, residues 19–23 and residues 29–37; one section of α-helix, residues 46–53, and chain reversals (β-turns) beginning at residues 3, 6, 10, 15, 27, 37, and 40. The predicted α-helical segment also has a high $\langle P_\beta \rangle$ value, and thus, some type of β-structure may be available as a viable alternative to the favored α-segment. Circular dichroism (CD) studies have indicated the solution structure of mEGF to contain approximately 22% β-structure and no α-helicity, with the remaining portion of its gross structure existing in an aperiodic conformation (Holladay et al., 1976; Taylor et al., 1972).

The solution structure of mEGF has recently been investigated by proton nuclear magnetic resonance (NMR) and photo-CIDNP (De Marco et al., 1983) and nuclear Overhauser (NOE) techniques at 500 MHz (Mayo, 1984). NOE studies have identified at least five or six α-CH proton resonances associated with α-CH protons to be involved in tiered β-sheet structure. Other nuclear Overahuser data have strongly suggested proximity relationships among Tyr-3, -10, and -13, His-22, and Ile-23. Such proximity relationships derived from these NOE data have allowed aspects of the tertiary structure (i.e., backbone folding) based on the Chou–Fasman predicted secondary structure to be deduced (Mayo, 1984). De Marco et al. (1983) have suggested, on the basis of photo-CIDNP experiments, that four of the five tyrosines and both tryptophans present in mEGF are solvent exposed.

This present study continues an on-going NMR investigation of the solution structure of mEGF and investigates 13 long-lived, amide proton resonances (i.e., those with lifetimes greater than ~5 min) by, principally, nuclear Overhauser (NOE) and 2D NMR COSY techniques. The virtue of the NOE technique (Noggle & Shirmer, 1971) is that it permits all major dipolar interproton interactions of an amide proton in a molecule to be detected. This allows one to identify those pairs of protons that are physically close together, and this information is useful both in making resonance assignments and in determining conformation. Similarly, most scalar coupled protons in a molecule can be identified in a single experiment by using two-dimensional J spectroscopy (COSY) (Bax & Freeman, 1981). Here, correlation of the NOE and 2D COSY data has been used to make assignments of various proton resonances in the NOE difference spectra and to obtain qualitative information regarding aspects of the most probable conformational state of mEGF in solution.

Materials and Methods

Mouse epidermal growth factor (mEGF), purified from mouse salivary gland extracts by the method of Savage & Cohen (1972), was provided by Professor Stanley Cohen, Vanderbilt University. Purity was checked by amino acid analysis, gel electrophoresis, and proton NMR.

Samples for ^{1}H NMR measurements had been lyophylized from H_2O solutions and redissolved in D_2O immediately before the experiment. The final protein concentration was about 0.6 mM in approximately 10 mM potassium phosphate buffer. The pD was adjusted by adding microliter increments of NaOD or D_3PO_4 to a 0.5-mL sample. All measurements were done at the pD value indicated in the text read directly from the pH meter and not adjusted for isotope effects (Kalinichenko, 1976; Bundi & Wüthrich, 1979).

^{1}H NMR spectra were recorded in the Fourier mode on a Bruker WM-500 spectrometer at 303 K. The solvent deuterium signal was used as the field-frequency lock. All chemical shifts are quoted in parts per million (ppm) downfield from sodium 4,4-dimethyl-4-silapentanesulfonate (DSS). The exchange rates of the amide protons for deuterium of the deuterium oxide solvent were determined by measuring the time-dependent decrease of resonance intensities as protons were replaced by deuterons. The areas of resonances were measured and calibrated relative to the area of the Tyr-III (3,5) proton resonance. The accuracy of these measurements is estimated to be for the most part better than ±10%. The experimental decay of the resonances was plotted as pseudo-first-order kinetics.

NOEs were generated by irradiating the desired peak for 0.8 s at a power level sufficient to null z magnetization of the irradiated peak in 0.05 s. A 2-ms delay was introduced before accumulation to reduce transient effects, and a time of 3.5 s was allowed between the beginnings of accumulations to allow for recovery of z magnetization. Difference spectra were obtained by subtracting the free-induction decay (FID) of the irradiated peak spectrum from the FID of a control spectrum that had been irradiated in a region where no resonances occur under the same experimental conditions.

The basic pulse sequence for the 2D homonuclear J-correlated (COSY) experiment is (Aue et al., 1976)

$$(P_1\text{–}t_1\text{–}P_2\text{–}t_2\text{–}D_5)_n$$

where P_1 and P_2 indicate 90° pulses, t_1 is the evolution period between the two pulses during which the various magnetization components are labeled with their characteristic frequencies, t_2 is the time during which the signal is recorded, and D_5 is the delay between successive acquisitions to allow for spin–lattice relaxation. In this particular experiment, the second pulse, P_2, was 45°, which has the effect of reducing the intensity of near-diagonal components. Axial peaks were suppressed by a 16-step phase-cycling routine; quadrature detection was used in both dimensions, and the carrier frequency was placed at the center of the spectrum. Data processing was done on a VAX 11785 computer system with software supplied by Dennis Hare, Columbia University. Other details are given in the figure caption for the COSY spectrum.

Results

Long-Lived Amide Protons in mEGF. Following solvation of H_2O-exchanged, lyophilized mouse epidermal growth factor (mEGF) in deuterium oxide, labile amide protons with lifetimes greater than the sample preparation time of approximately 5 min demonstrate their respective resonances in the

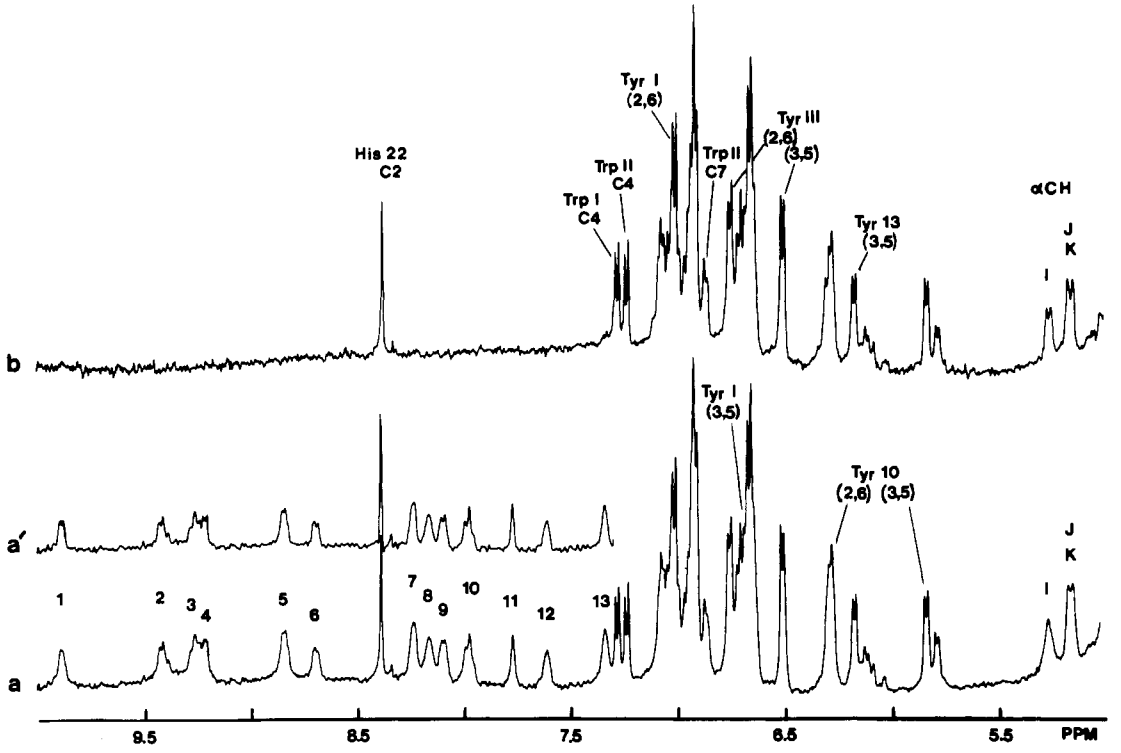

FIGURE 1: The 500-MHz proton NMR spectrum of the downfield proton region (5.0–10.0 ppm) in mEGF at pH 5.9 and 303 K. (a) Spectrum accumulated immediately after solvation of H_2O-exchanged, lyophilized sample in D_2O (long-lived amide proton resonances are present), (a') resolution-enhanced spectrum of the amide proton region (i.e., the data have been processed with a Lorentzian to Gaussian transformation to improve resolution), and (b) spectrum taken following exchange of long-lived amide protons for deuterium of the D_2O solvent. These spectra represent the time-averaged accumulation of 256 scans taken over approximately 12 min with a 90° pulse on a 0.4-mL sample at concentrations of 0.7 mM mEGF in 10 mM KH_2PO_4. The spectra (1a and 1b) are line broadened (exponential multiplication) by 1 Hz. Amide proton resonances are labeled as described in the text, and aromatic proton resonances are labeled as described in De Marco et al. (1983) and in Mayo (1984).

downfield region (i.e., 5.0–10.0 ppm) of an NMR spectrum (500 MHz) (Figure 1a). The long-lived amide protons number 13 and have their respective resonances labeled numerically from 1 to 13 from downfield to upfield, respectively (Figure 1a). Each number refers to a single amide proton resonance. Figure 1b presents a spectrum showing those resonances associated with the aromatic amino acid protons that are present following exchange of all amide protons for solvent deuterons. The aromatic amino acid proton resonances have been previously assigned (De Marco et al., 1983; Mayo, 1984). Some of these assignments are given in Figure 1.

Long-lived exchangeable amide proton resonances normally have been associated either with amide protons not readily solvent exposed (i.e., buried in the interior of the pattern) or with hydrogen-bonded amide protons. The latter explanation is favored in this case since a polypeptide of this size (i.e., 53 amino acid residues) would not be expected to have an extensive non-solvent-exposed region in which amide protons could be buried.

Any of these 13 amide proton resonances could be associated with the side-chain amide protons of the four arginines, the one glutamine, the three asparagines, or any of the 53 backbone amide protons present in mEGF. For these hydrogen-bonded amide protons, the kinetics of amide proton exchange for deuterons of the deuterium oxide solvent allow one to distinguish among these possible types of amide protons (i.e., side chain or backbone). Amide protons whose resonances are observed here display pseudo-first-order exchange rate constants on the order of 10^{-5} s^{-1} as indicated in Table I. Under the conditions in which these exchange experiments have been performed (i.e., pH 5.9 and 303 K), rates of exchange for arginine, glutamine, or asparagine side-chain amide protons would be 3–4 orders of magnitude greater than those rates observed here (Englander et al., 1972; Arnett, 1963; Eigen, 1964). This previous statement is strictly valid for solvent-accessible protons only. The apparent lifetimes of these 13 amide protons, furthermore, indicate rates of exchange observed for hydrogen-bonded backbone amide protons in other proteins involved in some type of secondary or tertiary structure (i.e., α-helical or β-sheet, etc.) (Wüthrich et al., 1980; Wüthrich & Wagner, 1979; Knox & Rosenberg, 1980; Rosa & Richards, 1979, 1981; Englander et al., 1980). These data, therefore, suggest that these amide proton resonances are associated with backbone amide protons conformed in some type of hydrogen-bonded, secondary or tertiary structure in mEGF.

Resolution enhancement of these backbone amide proton

Table I: Long-Lived Amide Proton Exchange Rates

amide proton resonance	chemical shift	pseudo-first-order rate constants, k_m ($\times 10^{-5}$ s^{-1})[a]	$J_{NH\alpha\text{-}CH}$ coupling constant (Hz)[b]
1	9.82	10	8
2	9.35	13	10
3	9.24	14	10
4	9.15	32	7.5
5	8.78	10	6
6	8.63	22	8
7	8.18	7	<5
8	8.10	7	<5
9	8.04	14	8.5
10	7.92	10	8.5
11	7.71	65	<5
12	7.55	10	<5
13	7.28	10	<5

[a] Measured at pH 5.9 and 303 K in 10 mM potassium phosphate buffer. [b] Approximate peak to peak coupling constant; actual coupling constant will be somewhat larger.

resonances (Figure 1a′) shows several of them to have resolvable proton–proton coupling constants (i.e., $J_{NH\alpha\text{-}CH}$) of 7 Hz or more (i.e., resonances 1–6, 9, and 10). From the theoretical Karplus relationship of the NHα-CH coupling constant on the dihedral angle and from experimental correlation of the X-ray crystallographic structure of bovine pancreatic trypsin inhibitor (BPTI) with the NMR NHα-CH coupling constants [Billeter et al., 1982; Wüthrich et al., 1982; Wüthich et al. (1980) and references cited therein], NHα-CH coupling constants of 7 Hz or greater observed here for mEGF indicate that at least these resonances are associated with backbone amide protons existing in some type of β-structure. Furthermore, since circular dichroism (CD) studies on mEGF (Holladay et al., 1976) indicate the presence of only β-structure and no α-helical structure, a high probability exists that other amide proton resonances observed here are also associated with backbone amide protons conformed in some type of β-structure.

Amide proton resonances 3 and 10, furthermore, appear to be triplet resonances and may therefore be tentatively assigned to glycine amide protons of which there are six in the primary structure of mEGF. It can also be observed in Figure 1 that α-CH proton resonance I in the absence of any amide proton resonances (Figure 1b) exists as an apparent doublet resonance while in their presence (Figure 1a) resonance I seems to belong to a higher order spin system. This information clearly suggests that α-CH proton resonance I is spin-coupled to one of these 13 long-lived backbone amide proton resonances.

Nuclear Overhauser Experiments. In order to evaluate the structural origin of these hydrogen-bonded backbone amide protons and perhaps to establish proximity relationships among them and to assign resonances, selective nuclear Overhauser experiments were performed on all 13 amide resonances shown in Figure 1a. The use of the nuclear Overhauser effect (NOE) in the structural characterization of a number of proteins (e.g., BPTI and lysozyme) has been well documented and correlated with internuclear distances taken from X-ray crystallographic data (Wüthrich et al., 1980; Dubs et al., 1979; Pulsen et al., 1980). The magnitude of NOEs observed at other proton resonances when a backbone amide proton resonance is irradiated is usually diagnostic of the type of structure in which that backbone amide proton exists (Wüthrich et al., 1982; Billeter et al., 1982). Such NOE data often permit the assignment of an amide proton resonance to a particular amino acid residue, especially when correlated with information that identifies scalar coupled resonances to be discussed later. In this way, proximity relationships derived from NOE data also provide a means for proposing and testing structural models of mEGF.

NOE difference spectra taken at pH 3.8 and 303 K and obtained by subtracting spectra with rf irradiation on and off a resonance of interest for 0.8 s are given in Figures 2a–h and 3a–f. The data presented in Figures 2 and 3 have identical resonances both interconnected with solid lines and similarly shaded.

NOEs observed on irradiation of the Tyr-III (2,6) proton resonance (i.e., Figure 2a) suggest proximity of three backbone amide protons (i.e. 4, 7, and 9) to α-CH I and Tyr-III. Proximity of Tyr-III and α-CH I has been previously observed (Mayo, 1984). Two upfield NOEs at resonances F1a and F1d have also been observed on irradiation of α-CH proton resonance I [i.e., called I1 and I3, respectively, in Mayo (1984)]. Resonance I1 (i.e., F1a) had been identified as the α-CH proton opposite to α-CH proton I in an antiparallel β-sheet structural region in mEGF, and resonance I2 (i.e., F1d) had been identified as arising from the β-CH_2 protons belonging to the same residue as α-CH I (Mayo, 1984). It seems likely, therefore, that resonances F1a and F1d are identical with resonances I1 and I2, respectively, in Mayo (1984).

The inverse NOE experiments, performed by irradiation of amide proton resonances 4, 7, and 9 (spectra b, c, and d, respectively, of Figure 2), confirm the proximity of these three amide protons (i.e. 4, 7, and 9) to Tyr-III and α-CH I. The magnitude of the NOE at α-CH proton resonance I on irradiation of the β-sheet backbone amide proton resonance 4 (Figure 2b) suggests, furthermore, that the α-CH proton I is the β-sheet N-terminal, α-CH proton of amide proton 4. Resonance 4b is likely identical with resonance F1d and, therefore, with resonance I2 in Mayo (1984). Comparison of these four NOE difference spectra (i.e., Figure 2a–d) indicates several other identical upfield resonances. NOEs at resonances J and 4c (Figure 2b) are likely the result of direct saturation of amide proton resonance 3.

The next set of four NOE difference spectra (i.e., Figure 2e–h) suggests proximity of four more amide protons (i.e., 3, 10, 11, and 13) to that structural domain involving Tyr-III and amide protons 4, 7, and 9. Additional structural information is given by irradiation of amide proton resonance 11 (Figure 2g), which suggests proximity of Trp-II to amide proton 7 and Tyr-III. An NOE at resonance 11h, the Ile-23 δ-CH_3 resonance (Mayo, 1984), also suggests proximity of Ile-23 to this same structural domain.

Irradiation of amide proton resonance 3 (Figure 2f) shows NOEs at amide proton resonance 10 and at α-CH proton resonances J and 3a as well as at several upfield resonances. On irradiation of α-CH proton resonance J (Mayo, 1984), NOEs were observed at α-CH proton resonance 3a [i.e., J1 in Mayo (1984)] and at the upfield resonance positions of resonances 3c and 3d [i.e., J2 and J3, respectively, in Mayo (1984)] (Figure 2f). The α-CH proton associated with resonance J was structurally assigned to an antiparallel tiered β-sheet region in mEGF (Mayo, 1984). The appearance of an NOE of such magnitude at α-CH proton resonance J on irradiation of amide proton resonance 3 (Figure 2f) suggests that the α-CH proton associated with resonance J is the β-sheet N-terminal α-CH proton neighboring amide proton 3 in this tiered β-sheet region.

Figure 3 presents the final six amide proton NOE difference spectra. Irradiation of amide proton resonance 2 (Figure 3a) shows NOEs at amide proton resonance 5, the Tyr-3 (3,5) proton resonance, α-CH proton resonance J, and α-CH proton resonance 2b, as well as at several other resonance positions upfield of the HDO resonance. Resonance 2e appears at the same chemical shift position as resonance J2 in Mayo (1984), observed on irradiation of α-CH proton resonance J. NOEs at α-CH proton resonance J were also observed on irradiation of amide proton resonances 3 and 10 (spectra f and g, respectively, of Figure 2). Furthermore, irradiation of amide proton resonance 3 (Figure 2f) shows NOEs at identical resonance positions as resonances 2b and 2e (Figure 3a) (i.e., resonances 3a and 3c, respectively, in Figure 2f).

Irradiation of amide proton resonance 5 shows, likewise, NOEs at amide proton resonance 2 and at the Tyr-3 (3,5) proton resonance. NOEs at several α-CH proton resonances (i.e., K, 5b, 5c, and 5d) among other upfield resonances are also noted. Proximity of α-CH K to Tyr-10 and Tyr-13 and the region around Tyr-3 has already been observed on irradiation on α-CH proton resonance K (Mayo, 1984). Furthermore, resonances 5d and 5e occur at identical resonance positions as resonances 1a [observed on irradiation of the

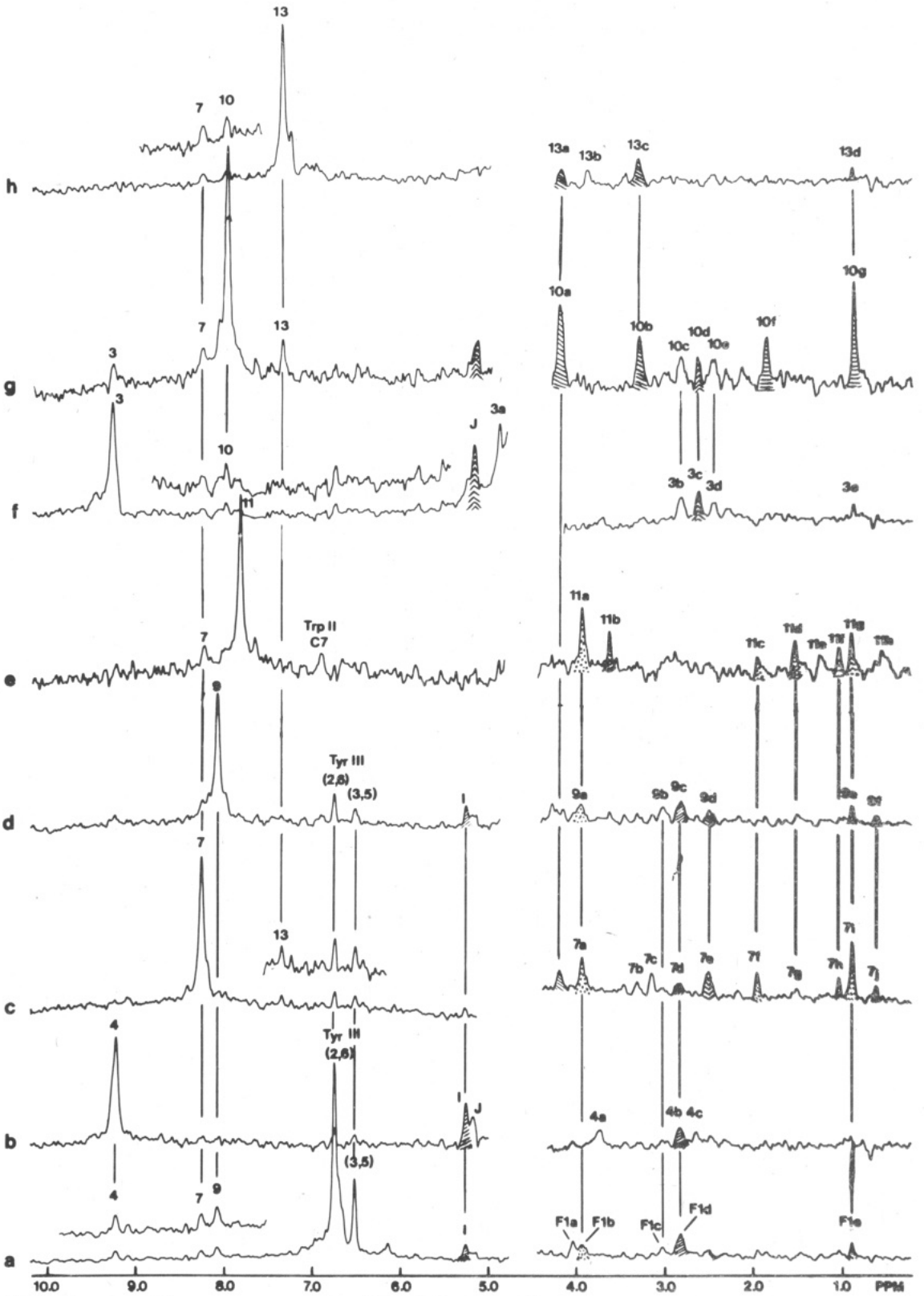

FIGURE 2: NOEs given by amide proton resonances in mEGF. Eight NOE difference spectra are shown, each representing the difference between an accumulation of 384 FIDs taken with saturating radio-frequency (rf) off-resonance and another accumulation of 384 FIDs taken with saturating radio-frequency on-resonance. In each case, the rf saturation time was 0.8 s. Spectra are for saturation of the Tyr-III (2,6) proton resonance (a) and for amide proton resonances 4 (b), 7 (c), 9 (d), 11 (e), 3 (f), 10 (g), and 13 (h). Labeling of resonances is as in Figure 1 and as described in the text. Sample conditions are as described in Figure 1, except at pH 3.8.

Tyr-10 (2,6) proton resonance] and H2b [observed on irradiation of the Tyr-10 (3,5) proton resonance], respectively, reported in Mayo (1984). α-CH proton K was already suggested to exist in some type of β-sheet structure (Mayo, 1984). Structurally, therefore, these data suggest proximity of Tyr-3 and the β-sheet amide protons associated with resonances 2 and 5 to the tiered β-sheet domain described above involving amide protons 3 and 10.

The amide protons associated with resonances 1, 6, and 12 (2.e., spectra c, e, and d, respectively, of Figure 3) are clearly

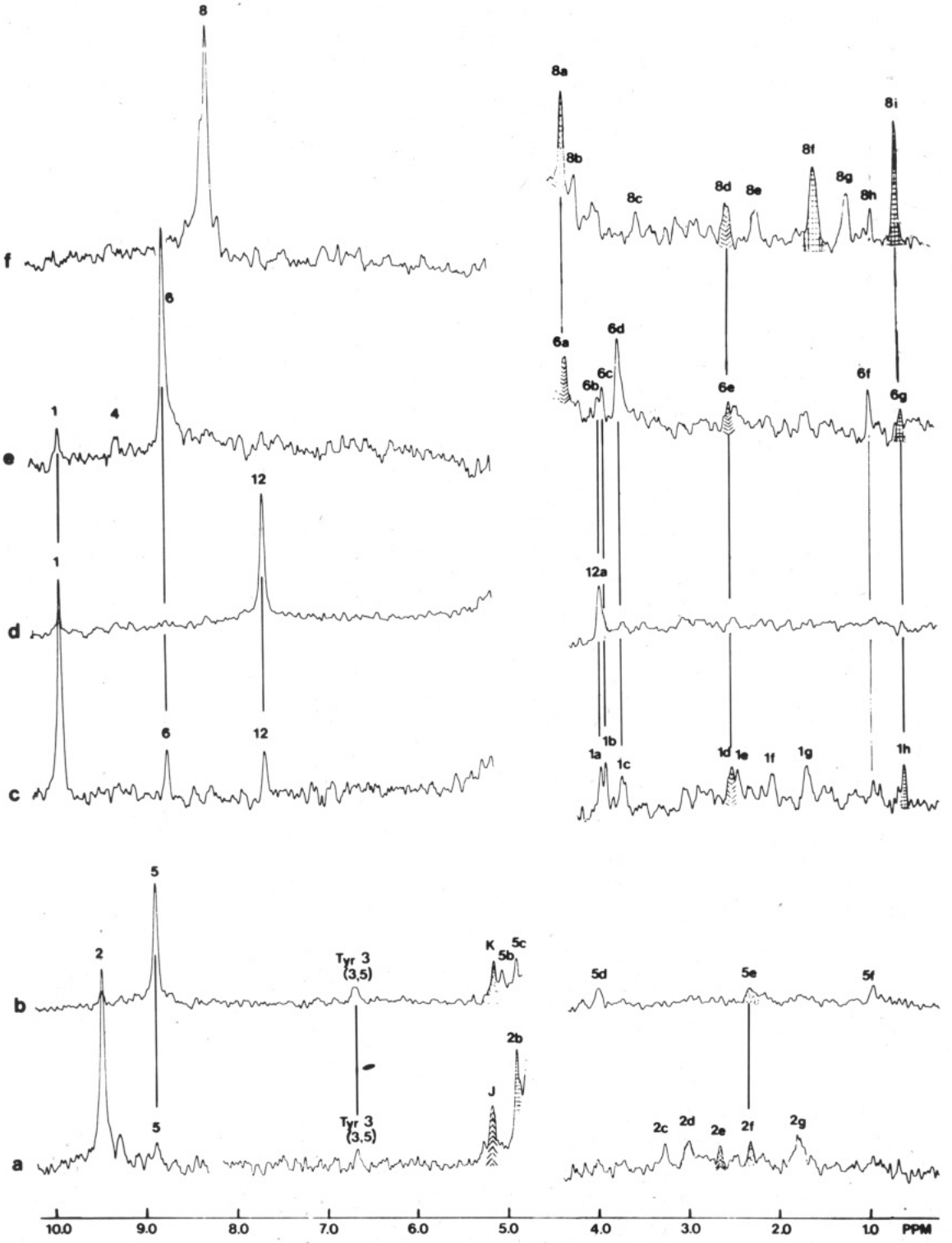

FIGURE 3: NOEs given by amide proton resonances in mEGF. Six NOE difference spectra are shown with accumulations as described in Figure 2. Spectra are for saturation of amide proton resonances 2 (a), 5 (b), 1 (c), 12 (d), 6 (e), and 8 (f). Sample conditions are as described in Figure 2.

proximal to one another as evidenced by apparent NOEs at their respective resonance positions. Among these NOE spectra, several identical upfield resonances are also apparent. Furthermore, irradiation of amide proton resonance 6 gives an NOE at amide proton resonance 4, and on irradiation of NH resonance 4 (Figure 2b), an NOE was also observed at resonance position 6d. Structurally, these data suggest proximity of amide proton 6 and the region containing amide protons 1 and 12 to that region around amide proton 4 and Tyr-III. As with other amide proton resonances investigated here, the magnitudes of NOEs at α-CH resonance positions observed on irradiation of these amide proton resonances (i.e. 1, 6, and 12) are also suggestive of β-sheet structure.

Irradiation of amide proton resonance 8 (i.e., Figure 3f) demonstrates no apparent NOEs at other downfield amide or aromatic proton resonances, although inspection of the upfield resonances in Figure 3f indicates that several resonances (e.g., 8a, 8d, and 8i) occur at identical resonance positions as resonances shown in Figure 3c, e (i.e., resonances 6a, 6e (1d), and 6g (1h), respectively). The magnitude of an NOE at α-CH proton resonance 8a, furthermore, indicates that amide proton 8 also exists in a β-sheet structure; the α-CH proton

8a probably belongs to the N-terminal amino acid residue of amide proton 8. This information, therefore, suggests that amide proton 8 also somehow belongs to this tiered β-sheet domain.

In summary, these NOE results render desired structural information and suggest that these 13 long-lived, backbone amide protons exist in one and the same tiered β-sheet structural domain in mEGF. This structural domain contains Tyr-III, Trp-II, Tyr-3, and Ile-23.

2D NMR COSY Experiment. In regard to a structural elucidation of this tiered β-sheet domain in mEGF, the presence of proximity relationships among protons associated with resonances in an NMR spectrum is only made meaningful if some or all of these resonances have been assigned either to specific amino acid residues in the sequence or to a particular amino acid residue type. Resonances present in that region of an NMR spectrum upfield of the HDO resonance are usually so convoluted that assignment of these resonances by normally employed one-dimensional NMR spectroscopic techniques (e.g., NOE or spin-decoupling experiments) is highly improbable. With the advent of 2D NMR spectroscopy (Jeener, 1971; Aue et al., 1976), a powerful means of deconvoluting and assigning resonances present even in this highly convoluted upfield region was at hand. The use of 2D NMR techniques in studying proteins has been discussed at some length by Wüthrich et al. (Nagayama & Wüthrich, 1981; Wagner et al., 1981). A 2D NMR COSY (i.e., correlated spectroscopy) experiment (Aue et al., 1976) performed on mEGF is shown in Figure 4 for the upfield region and in Figure 5 for the amide proton region. These data inform us which resonances are scalar coupled. The diagonal in the two-dimensional spectrum in Figure 4 running from the bottom left to the top right represents a cross-section thru a normal one-dimensional NMR spectrum shown across the bottom of this 2D plot. The off-diagonal cross-peaks in this presentation represent spin-coupled resonances as indicated by the connected lines drawn in Figures 4 and 5 for resonances to be discussed. From these data, spin-coupled resonances may be tentatively assigned to specific amino acid residues on the basis of their chemical shifts. Furthermore, resonances present in the amide proton NOE difference spectra shown previously (i.e., Figures 2 and 3) can be correlated to these spin-coupled resonances in the COSY experiment with the goal of possibly assigning resonances in the NOE difference spectra and identifying proximity relationships between various amino acid residues. This final assimilation of NOE and 2D COSY data, at the very least, has the potential of limiting possible models for the tiered β-sheet structural domain involving the previously described long-lived amide protons.

Spin-Coupled Resonances and Resonance Assignments in the NOE Difference Spectra. In the following section, tentative assignments of probable spin-coupled resonances to protons of an amino acid residue have been based on the reference chemical shift data taken from Bundi & Wüthrich (1979) and references cited therein. These reference chemical shift data (Bundi & Wüthrich, 1979) were compiled from proton NMR studies on the synthetic tetrapeptide H-Gly-Gly-X-Ala-OH, where X stands for the amino acid residue of interest. Variations in observed chemical shifts due to amino acid sequence differences have been estimated by these authors (Bundi & Wüthrich, 1979) to be on the order of ±0.05 ppm in the absence of aromatic ring current fields. Other chemical shift reference data from native proteins have also been used: cytochrome (McDonald & Phillips, 1973) and BPTI (Wüthrich et al., 1980, 1982). Since conformational perturbations on observed chemical shifts may also play a role, these reference data are used here only as a rough guideline for tentative amino acid assignments.

Since protons of a particular amino acid residue are clearly proximal to one another, it seems reasonable to assume that on irradiation in an NOE experiment of an amide proton resonance NOEs will be observed at one or more resonances associated with protons of a particular amino acid residue. The primary sequence of mEGF is shown in Figure 6 for ready reference to amino acid residues to be discussed in the following text.

Starting with the NOE difference spectrum shown in Figure 2a, one can ask the question which resonances may be spin coupled. Inspection of the 2D COSY data in Figure 4 indicates that α-CH proton resonance I and β-CH_2 proton resonance F1d are spin coupled. Amide proton resonance 9 is also spin coupled to α-CH resonance I (Figure 5). These resonances can be tentatively assigned to the Tyr-III α, β, and NH protons, respectively, since a greater than 90% probability exists that irradiation of a tyrosine 2,6-proton resonance will give NOEs of these magnitudes at its own residual proton resonances.

Amide proton resonance 4 is spin coupled to an α-CH resonance at 4.77 ppm, which in turn is spin coupled to resonance 4a in Figure 2b. The chemical shifts of these two upfield resonances in this spin system are characteristic of the α-CH (4.77 ppm) and β-CH_2 (3.73 ppm) protons of a serine residue. Resonances 4 and 4a are, therefore, tentatively assigned to the NH and β-CH_2 protons, respectively, of one of the six serine residues present in mEGF (i.e., Ser-2, -8, -9, -25, -28, and -38).

In Figure 2c, α-CH proton resonance 7a is spin coupled to NH proton resonance 7 as well as to β-CH_2 proton resonance 7f, which, in turn, is spin coupled to two methyl proton resonances 7h and 7i. The only amino acid spin systems with spin-coupled resonances at these chemical shift positions are those arising from a leucine, valine, or an isoleucine residue. Furthermore, resonances 7h and 7i are apparent doublet resonances; thus, negating isoleucine as a possible candidate since an isoleucine residue would not be expected to have two doublet resonances spin coupled to one other resonance. There are four leucines (i.e., Leu−15, −16, −47, and −52) and two valines (i.e., Val−19 and −34) present in mEGF. Resonances 7g and 7j may also be spin coupled and belong to some other hydrophobic residue proximal to NH-7 and Tyr-III.

Resonance 11a, -c, -f, and -g in Figure 2e occur at identical resonance positions as resonances 7a, -f, -h, and -i, respectively, in Figure 2c, which are tentatively assigned to protons of a leucine or valine residue. Resonances 11b and 11d in Figure 2e are also probably spin coupled and, on the basis of their chemical shifts, are likely assignable to the δ- and γ-CH protons, respectively, of one of the four arginine residues (i.e., Arg-41, -45, -48, or -53) present in mEGF. Lysine would also have been a viable alternative to arginine; mEGF is, however, devoid of lysine residues (Savage et al., 1973). The probable α- and β-CH proton resonances of this arginine spin system are also indicated in Figure 4 at 3.93 and 1.66 ppm, respectively. Resonance 7a is also found at 3.93 ppm and may even be identified with this arginine α-CH resonance.

NH proton resonance 3 (Figure 2f) is spin coupled to α-CH proton resonance 3a. α-CH proton resonance J is most likely spin coupled to β-CH_2 proton resonance 3c, which in turn is spin coupled to γ-CH_2 proton resonance 3b. This spin system is typical for the α-CH, β-CH_2, and γ-CH_2 protons arising from a glutamic acid or glutamine residue.

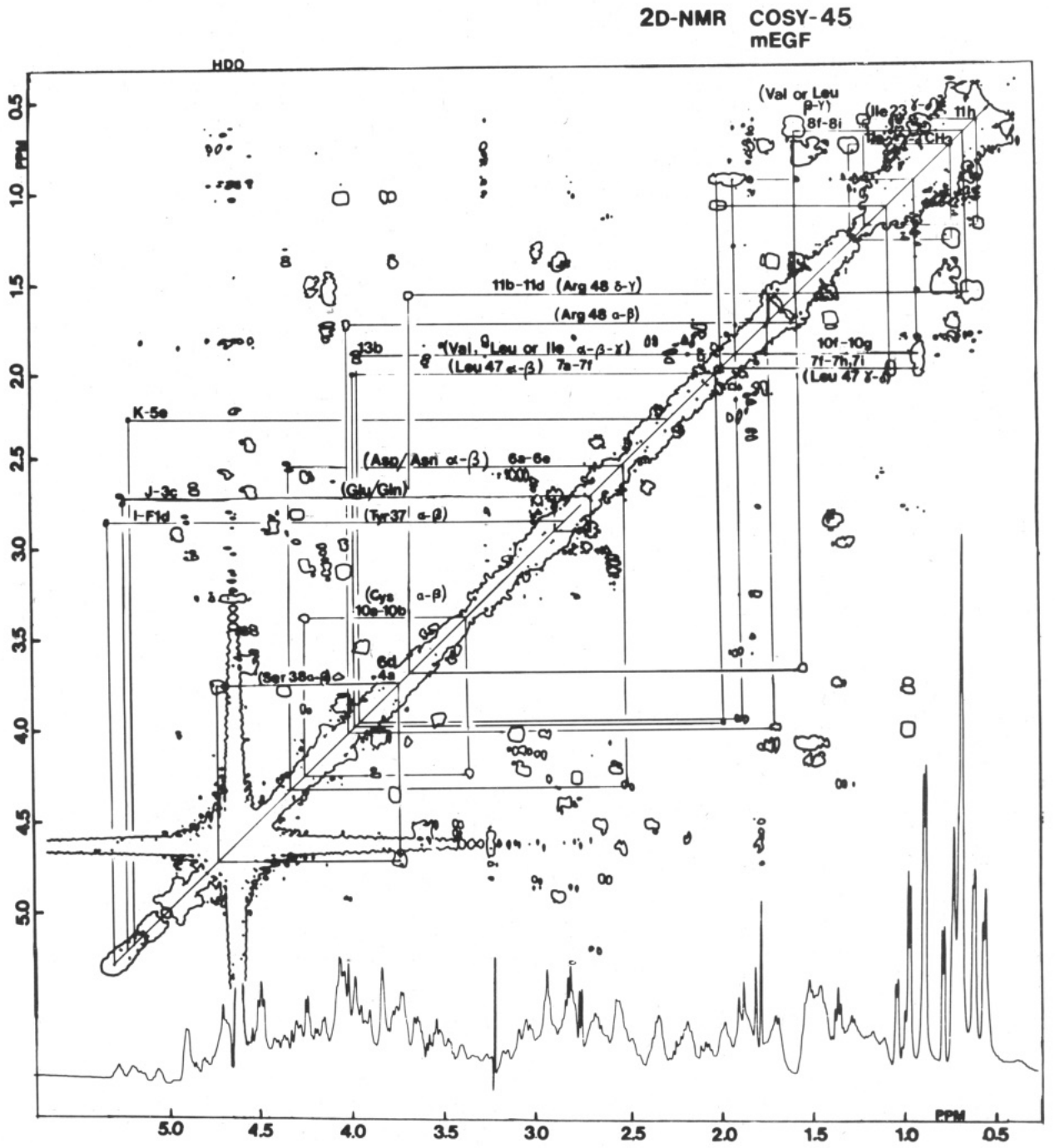

FIGURE 4: The 500-MHz COSY 45 spectrum (contour plot) (upfield region) of mEGF. The spectral width was ±2500 Hz. The data set consisted of 2048 points in the t_2 dimension and 512 points in the t_1 dimension; 144 FIDS were accumulated for each value of t_1, with a 1-s delay between acquisitions. A 90° pulse (12 μs) was used for the first pulse, but the second pulse was 6 μs (45°). The resulting data matrix was processed with a phase-shifted sine bell in both dimensions and was zero filled in the f_1 dimension. The absolute value mode is used. The data were processed on a VAX 11785 computer system with software supplied by Dennis Hare, Columbia University. Sample conditions are as described in Figure 2. Solid lines connect spin-coupled resonances through cross-peaks. The labels above the solid lines refer to resonances in the NOE difference spectra and discussed in the text. Tentative assignments of these resonances to protons of a specific amino acid residue are given in parentheses and justified under discussion.

In Figure 2g, NH proton resonance 10 is spin coupled to α-CH proton resonance 10a. Since NH resonance 10 is a triplet resonance, it must, therefore, be identified as a glycine NH, and α-CH resonance 10a must be this glycine's α-CH_2 proton resonance. α-CH proton resonance 10a may even represent a second α-CH proton that may be spin-coupled to β-CH_2 proton resonance 10b. Resonances 10a and 10b occur in spectral regions typical for α-CH and β-CH_2 proton resonances, respectively, associated with cystine residues of which there are six in mEGF (i.e., Cys-6, -14, -20, -31, -33, and -42). Resonances 10f and 10g are also likely spin coupled and, on the basis of their chemical shifts, are probably assignable to β-CH and γ-CH protons, respectively, of still another hydrophobic residue (i.e., Val, Ile, or Leu). The α-CH proton resonance of this hydrophobic residue spin system probably occurs at 4.2 ppm (Figure 4).

NH proton resonance 2 (Figure 3a) is spin coupled to α-CH proton resonance 2b, which in turn may be spin coupled to β-CH_2 proton resonance 2d. NH proton resonance 5 (Figure 3b) is spin coupled to α-CH proton resonance 5c, while α-CH proton resonance 5b may be spin coupled to β-CH_2 proton resonance 2g.

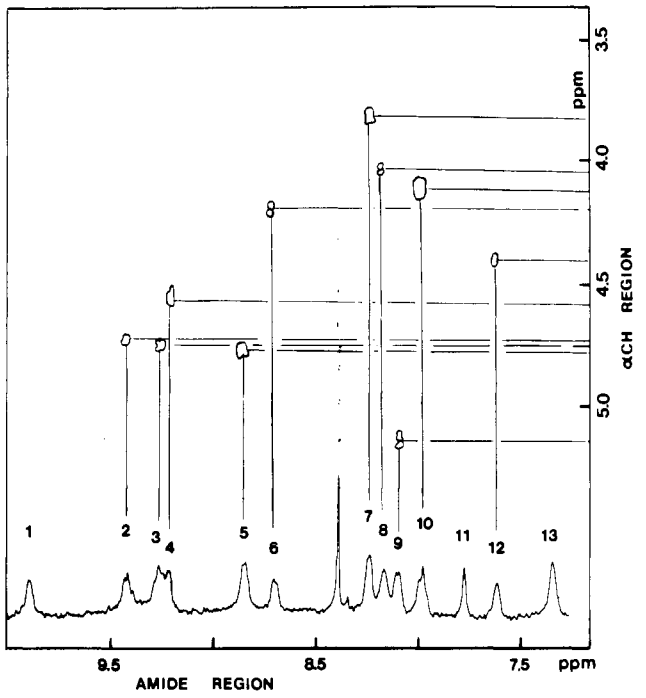

FIGURE 5: The 500-MHz COSY 45 spectrum (contour plot) (amide proton region) of mEGF. Conditions are the same as in Figure 2. Only the amide proton region showing spin-coupled resonance positions to the α-CH proton region is shown.

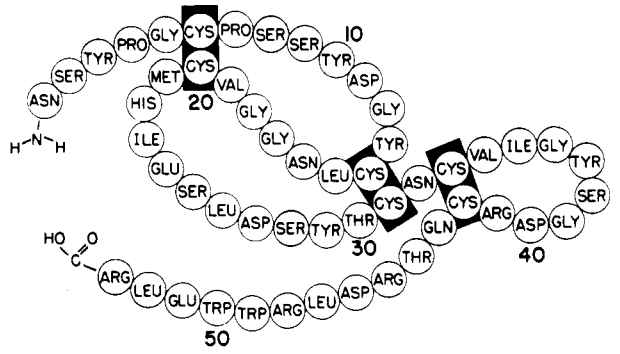

FIGURE 6: Primary sequence of mouse epidermal growth factor (mEGF) as presented by Savage et al. (1972). (Reprinted with the permission of the copyright holder.)

Several resonances occurring around 4 ppm in Figure 3c–e could be spin coupled as evidenced by the large number of cross-peaks in this region observed in Figure 4. The large number of anticipated spin coupled resonances in this spectral region, however, makes a definitive evaluation impossible. This spectral region is typical for threonine α-CH and β-CH proton resonances, as well as for serine β-CH_2 and glycine proton resonances. mEGF contains two threonine, six serine, and six glycine residues.

NH proton resonance 6 is spin coupled to α-CH proton resonance 6a, which is also spin coupled to β-CH_2 proton resonance 6e (Figure 3c). These α-CH and β-CH proton resonances (i.e., 6a and 6d) lie in chemical shift regions typical for α-CH and β-CH proton resonances, respectively, associated with an aspartic acid or arsparagine residue.

NH proton resonance 8 is spin coupled to α-CH proton resonance 8b. Resonances 8f and 8i (Figure 3f) are also likely spin coupled and are tentatively assignable to methylene and methyl protons, respectively, of another hydrophobic aliphatic residue.

These above-described tentative assignments are shown in Figures 4 and 5 with interconnecting lines and have been summarized in Table II. Probable spin-coupled resonances are also similarly shaded in the NOE difference spectra of Figures 2 and 3. Assignment of any of these resonances to a specific amino acid residue in the primary structure indicated in parentheses in Figure 4 will be justified under Discussion.

Table II: Resonance Assignments in the NOE Difference Spectra

proton resonance	chemical shift (ppm)	tentative assignment
Trp-I		Trp-50
Trp-II		Trp-49
Tyr-I		Tyr-29
Tyr-III		Tyr-37
I	5.25	Tyr-37 α-CH
Fid (4b, 7d, 9c)	2.82	Tyr-37 β-CH_2
9	8.04	Tyr-37 NH
4	9.15	Ser-38 NH
4a (6d)	3.73	Ser-38 β-CH_2
	4.77	Ser-38 α-CH
7	8.18	Leu-47 NH
7a (11a)	3.93	Leu-47 α-CH
7f (11c)	1.93	Leu-47 β-CH_2 and γ-CH_2
7h (11f)	1.0	Leu-47 δ-CH_3
7i (9e, 11g)	0.87	Leu-47 δ-CH_3
7g	1.5	β- or γ-CH_2 of a hydrophobic residue
7j	0.58	γ- or δ-CH_3 of a hydrophobic residue
J	5.16	α-CH probably of a Glu or Gln residue
3c (10d, 2e)	2.63	β-CH_2 probably of a Glu or Gln residue
3b (10c)	2.47	γ-CH_2 probably of a Glu or Gln residue
10	7.92	Gly-36 NH
10a (13a)	4.2	Gly-36 α-CH_2
10a	4.2	α-CH probably of a Cys residue
10b	3.32	β-CH_2 probably of a Cys residue
10f	1.85	β-CH_2 of a hydrophobic residue
10g	0.87	γ-CH_3 of a hydrophobic residue
13b	3.89	α-CH of a hydrophobic residue
11	7.71	Arg-48 NH
11b	3.63	Arg-48 δ-CH_2
11d	1.52	Arg-48 γ-CH_2
11e	1.22	β-CH_2 or γ-CH of a hydrophobic residue
11h	0.54	Ile-23 δ-CH_3
2	9.35	NH probably of an Asp or Asn residue
2b	4.82	α-CH probalby of an Asp or Asn residue
2d	2.99	β-CH_2 probably of an Asp or Asn residue
6	8.63	NH
6a (8a)	4.28	α-CH probably of an Asp or Asn residue
6e (8d)	2.50	β-CH_2 probably of an Asp or Asn residue

Discussion

Physical evidence for a tiered β-sheet structural domain in mouse epidermal growth factor (mEGF) has been presented. Proximity relationships derived from nuclear Overhauser effect (NOE) data strongly suggest that these 13 hydrogen-bonded, β-sheet backbone amide protons investigated here exist in this tiered, β-sheet domain, which includes Tyr-III and Trp-II and is proximal to Tyr-3. The pseudo-first-order exchange rate constants for these long-lived amide protons given in Table I also suggest that these amide protons exist in one and the same molecular domain. Furthermore, it is interesting to note that the number of β-sheet, backbone amide protons observed here (i.e., 13) represents 24–25% of the total number of backbone amide protons present in mEGF (i.e., 53 amino acid residues) and correlates well with the total amount of β-structure interpreted from circular dichroism (CD) studies on the protein (i.e., 22%) (Holladay et al., 1976; Taylor et al., 1972). On the basis of the Chou–Fasman algorithm for secondary structural predictions (Chou & Fasman, 1974a,b, 1978a,b) and model-building studies, Holladay et al. (1976) have found that a tiered β-sheet domain in mEGF may be formed from β-sheet segments of residues 29–37, residues 46–53, and residues 19–23. The present data support this prediction at least in part.

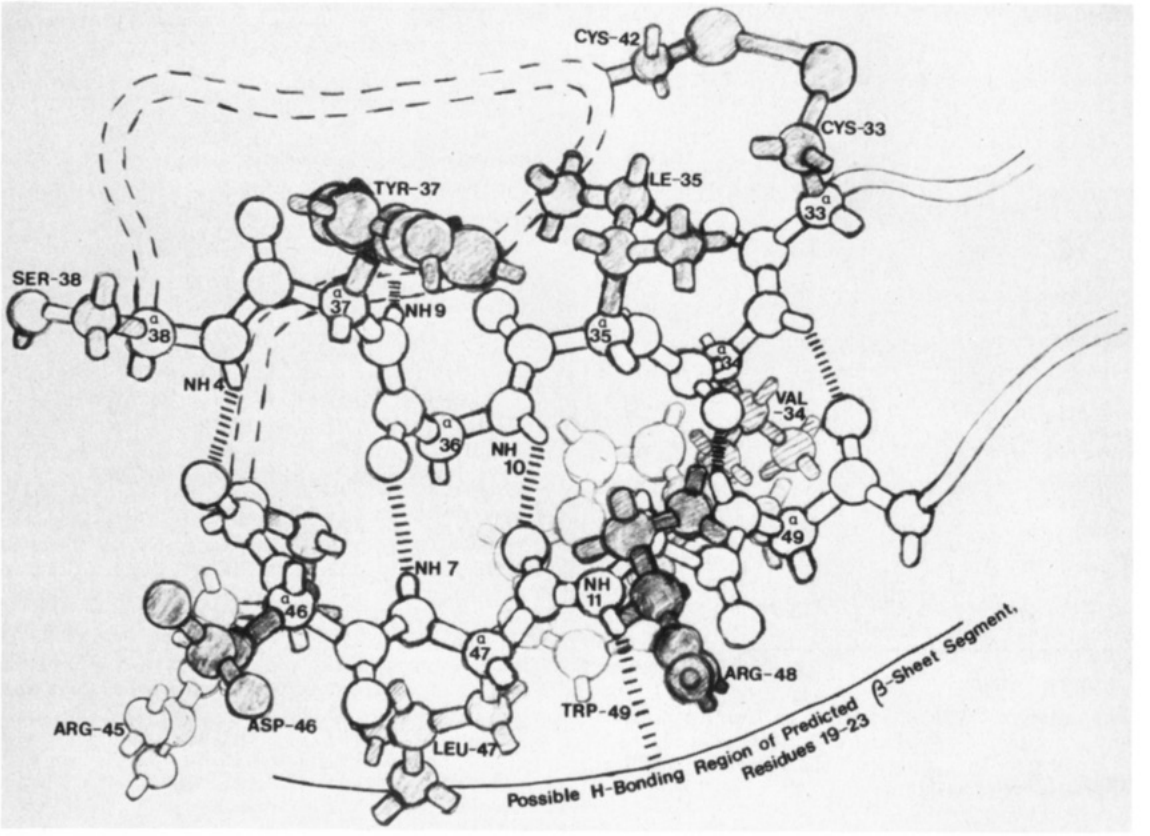

FIGURE 7: Proposed partial structure of the tiered β-sheet domain in mEGF. Key proximity relationships in mEGF are drawn for a particular molecular orientation. The model is based primarily on NOE data presented in this text. The error in the atomic positions shown could be as high as ± 2 Å.

NOE data involving amide and aromatic proton resonances and upfield resonances assigned on the basis of 2D COSY and chemical shift reference data provide a powerful tool for the elucidation of aspects of this β-sheet structural domain. On the basis of these nuclear Overhauser data, Tyr-III is suggested to be conformed within 3–4 Å of three amide protons (i.e., 4, 7, and 9). Tyr-III can be assigned to either Tyr-29 or Tyr-37 in mEGF (Mayo, 1984). Both Tyr-29 and Tyr-37 have been predicted by the secondary structural algorithm of Chou–Fasman to exist in an extended β-sheet conformation (Holladay et al., 1976). Furthermore, from previous NOE experiments on mEGF, Tyr-III has been suggested to exist in an antiparallel, β-sheet conformation (Mayo, 1984); therefore, on the basis of proximity arguments, it seems likely that the amide protons associated with resonances 4, 7, and 9 are also conformed in this tiered β-sheet conformation.

The observation of a strong NOE between serine amide proton resonance 4 and Tyr-III α-CH proton resonance I (Figure 2b) further supports this β-sheet structural assignment and suggests that a serine residue is present on the C-terminal side of Tyr-III in the primary structure of mEGF. In Figure 6 only one such dipeptide sequence is found with Tyr-37 and Ser-38. Tyr-III is, therefore, tentatively assigned to Tyr-37. Amide proton resonance 4 and β-CH_2 proton resonance 4a are likewise tentatively assigned to the NH and β-CH_2 protons, respectively, of Ser-38. By a process of elimination, Tyr-I can be assigned to Tyr-29, the only remaining unassigned tyrosine residue in mEGF (Mayo, 1984).

Amide proton 9 has been assigned to Tyr-37 (i.e., Tyr-III), which is proximal to the leucine or valine amide proton 7. NH-7 has, furthermore, been suggested as the N-terminal neighbor of the residue to which NH-11 belongs. Since NH-11 is proximal to a tryptophan and an arginine residue, the C-terminal segment of the protein running from residues 41 to residue 53 in which all tryptophan and arginine residues are located must, therefore, somehow be part of this tiered β-sheet domain near Tyr-37. To best explain these data, a partial structure of this domain is suggested in Figure 7. Part of this C-terminal segment is shown as an extent β-sheet chain running antiparallel to the Tyr-37 β-sheet segment. Doing this most easily brings a leucine, an arginine, and a tryptophan residue into proximity with Tyr-37. Accepting this partial structure allows tentative assignment of NH-7 to Leu-47 and NH-11 to Arg-48. Glycine NH-10 is also proximal to NH proton 7 and, therefore, to Tyr-37. Gly-36 is sequentially proximal to Tyr-37 and is, therefore, the prime candidate for assignment to the glycine residue of NH-10.

Additional structural information can be deduced from results concerning Tyr-37 (i.e., Tyr-III). From the data presented, it is clear that the Tyr-37 NH proton 9 is hydrogen bonded. Since Tyr-37 exists in a β-sheet conformation, the amide protons of the sequential residues associated with resonances 9 and 4 (or 10) must be present on opposite sides of the β-sheet segment containing Tyr-37. Structurally, therefore, these data suggest that hydrogen bonding exists on both sides of the β-sheet segment containing Tyr-37 as is shown in Figure 7.

If we accept the interpretation of these data discussed above and the basic tenets of the predicted secondary structure of mEGF (Holladay et al., 1976), we have arrived at the conformation shown in Figure 7. Sections of two predicted β-sheet segments (i.e., Tyr-29 to Tyr-37 and Asp-46 to Arg-53) are folded onto one another by two chain reversals (i.e., β-turns) beginning at Tyr-37 and at Asp-40. If we place these β-turns on the Tyr-37 NH proton side of its β-sheet segment and create a half-β-turn involving Thr-44, Arg-45, and Asp-46, the C-terminal β-sheet segment will run antiparallel to the Tyr-37 β-sheet segment allowing hydrogen-bond formation between

respective backbone carbonyls and amide protons to occur. The disulfide bridge between Cys-33 and Cys-42 (Savage et al., 1973) is also structurally accounted for by this model. It should be mentioned that internuclear positions shown in Figure 7 could be in error as much as ±2 Å, depending on such circumstances as, for example, the rotation of side groups and the exact positioning of the antiparallel β-sheet chains with respect to one another.

For the moment, it is impossible to continue the structural model of this tiered β-sheet domain any further than shown in Figure 7 without introducing an undesired level of ambiguity. This limitation is due primarily to a lack of spin-coupling information on the remaining resonances observed in the NOE difference spectra and/or to the inability to make a tentative assignment of spin-coupled resonances to a particular amide acid residue.

Other data presented in this study are, however, suggestive of further structural aspects of this tiered β-sheet domain. First of all, from the lack of NOEs at tryptophan proton resonance positions on irradiation of these tiered β-sheet amide proton resonances other than from irradiation of amide resonance 11, it may be suggested that at least part of the C-terminal segment is not involved in hydrogen bonding in this tiered β-sheet structure. Irradiation of backbone amide proton resonances located on the same chain as these tryptophan residues would be expected to give NOEs at tryptophan proton resonances, much the same as would be expected of tyrosine residues seen here, for example, with Tyr-37. De Marco et al. (1983) have, furthermore, indicated that both tryptophan residues are isotropically free, solvent exposed, and not trapped in any hydrophobic pockets; this observation would not be expected of a tryptophan residue whose backbone amide proton is H bonded in a tiered β-sheet structure. It may be then that past Arg-48 the remaining portion of the C-terminal segment extends into the solvent away from this tiered β-sheet domain.

A missing link between structural information on the N-terminal domain of mEGF previously investigated (Mayo, 1984) and this tiered β-sheet domain discussed above is provided by NOE data from NH resonances 2, 5, and 11. In Mayo (1984), proximity relationships based on NOE data were established among Tyr-3, Tyr-10, Tyr-13, His-22, and Ile-23, allowing aspects of the probable backbone folding of the N-terminal structural domain in mEGF to be suggested. On the basis of the predictive methods of Chou–Fasman, chain reversals (β-turns) at residues 3, 6, 10, and 15 were followed by a segment of β-sheet running from Val-19 to Ile-23, which allowed folding of the backbone such that Ile-23 and His-22 were proximal to Tyr-3. NOE data presented in this present study suggest proximity of NH-11, assigned to the Arg-48 backbone NH, to Ile-23. Furthermore, amide protons 2 and 5 are suggested to be proximal to Tyr-3 and protons previously assigned to this N-terminal domain as well as to protons assigned to this tiered β-sheet domain. Two major parts of the mEGF structural puzzle, therefore, may fit together as indicated at the bottom of Figure 7 as the possible H-bonding region of residues 19–23.

Lastly, it should be mentioned that, aside from Ile-23 and Leu-47, a minimum of four other hydrophobic aliphatic residues (i.e., Leu, Val, and Ile residues) represented by resonances 7g–j, 11e, 10f–g, and 8f–i in the NOE difference spectra are present in this tiered β-sheet region. Since two isoleucine, two valine, and four leucine residues are present in mEGF, these data would then suggest that the majority of these aliphatic hydrophobic residues are conformed in this tiered β-sheet region. In Figure 7, Ile-35 and Val-34 stand out as possible candidates for assignment to some of the resonances mentioned above. The lack of chemical shift dependence on pH (i.e., from approximately pH 3.5 to pH 6.0) for most of these 13 amide proton resonances, moreover, suggests the absence of Asp and Glu residues from this domain (K. H. Mayo, unpublished results). Further investigations of this tiered β-sheet region as well as a complete structural elucidation of mEGF are presently under way by using 2D NMR techniques.

In regard to structure–function relationships in mEGF, little can be said at this point in time. It is interesting to note, however, that most of the residues involved in this tiered β-sheet domain are hydrophobic and, at least in the case of Tyr-37 and Trp-49, are also solvent exposed (DeMarco et al., 1983). Primarily on the basis of X-ray crystallographic data on insulin, another well-known protein hormone, such a structurally well-defined hydrophobic region has been suggested as the insulin receptor binding site (Blundell et al., 1971, 1972; Blundell, 1975; Pullen et al., 1976). Furthermore, since epidermal growth factor isolated from human sources (i.e., hEGF) (Cohen & Carpenter, 1975; Gregory, 1975) has been shown to exhibit the same biological activities and receptor binding properties as mEGF in a variety of tissues (Hollenberg & Cuatrecasas, 1973, 1975; O'Keefe et al., 1974; Carpenter et al., 1975) as well as share a common receptor site in cultured human fibroblasts (Hollenberg & Gregory, 1977), it seems feasible to suggest that the structure of mEGF and hEGF are very similar if not identical even though their amino acid sequences differ at 16 positions (Gregory & Preston, 1977). No independent structural data is yet available on human EGF. However, assuming their structures to be nearly identical and comparing their sequences in terms of the structural data presented here on mEGF, all residues in this proposed tiered β-sheet structural domain have been conserved in the human species while other segments of the primary structure vary widely; the N-terminal segment (i.e., residues 1–17), for example, contains several nonconservative substitutions (i.e., hydrophobic residues replaced by charged ones). On the basis of the information given above, this tiered β-sheet structural domain in mEGF may, in fact, be the protein hormone's receptor binding domain.

ACKNOWLEDGMENTS

Prof. Stanley Cohen, Vanderbilt University, is gratefully acknowledged for provision of mouse epidermal growth factor (mEGF). Many special thanks to Prof. J. H. Prestegard for his support and guidance and for many helpful discussions. Josef W. Mayo is also gratefully acknowledged for assistance with the preparation of figures.

Registry No. EGF, 62229-50-9.

REFERENCES

Arnett, E. M. (1963) *Prog. Phys. Org. Chem. 1*, 223–278.
Aue, W. P., Bartholdi, E., & Ernst, R. R. (1976) *J. Chem. Phys. 64*, 2229.
Bax, A., & Freeman, R. (1981) *J. Magn. Reson. 44*, 542.
Billeter, M., Braun, W., & Wüthrich, K. (1982) *J. Mol. Biol. 152*, 321–345.
Blundell, T. L. (1975) *New Sci. 18*, 662–664.
Blundell, T. L., Cutfield, J. F.; Cutfield, S. M., Dodson, E. J., Dodson, G. G., Hodgkin, D. C., Mercola, D. A., & Vijayan, M. (1971) *Nature (London) 231*, 506–511.
Blundell, T. L., Dodson, G. G., Hodgkin, D. C., & Mercola, D. A. (1972) *Adv. Protein Chem. 26*, 279–402.

Buhrow, S. A., Cohen, S., & Staros, J. V. (1982) *J. Biol. Chem. 257*, 4019–4022.
Buhrow, S. A., Cohen, S., Garbers, D. L., & Staros, J. V. (1983) *J. Biol. Chem. 258*, 7824–7827.
Bundi, A., & Wüthrich, K. (1979a) *Biopolymers 18*, 279–285.
Bundi, A., & Wüthrich, K. (1979b) *Biopolymers 18*, 285–297.
Carpenter, G., & Cohen, S. (1976) *J. Cell. Biol. 71*, 159–171.
Carpenter, G., & Cohen, S. (1979) *Biochemical Actions of Hormones*, Vol. V, Academic Press, New York.
Carpenter, G., Lemback, K. J., Morrison, M. M., & Cohen, S. (1975) *J. Biol. Chem. 250*, 4297–4303.
Chou, P. Y., & Fasman, G. D. (1974a) *Biochemistry 13*, 211–221.
Chou, P. Y., & Fasman, G. D. (1974b) *Biochemistry 13*, 222–245.
Chou, P. Y., & Fasman, G. D. (1978a) *Annu. Rev. Biochem. 47*, 251–276.
Chou, P. Y., & Fasman, G. D. (1978b) *Adv. Enzymol. Relat. Areas Mol. Biol. 48*, 45–148.
Cohen, S. (1962) *J. Biol. Chem. 237*, 1555–1562.
Cohen, S. (1965) *Dev. Biol. 12*, 394–407.
Cohen, S., & Elliott, G. A. (1963) *J. Invest. Dermatol. 40*, 1–5.
Cohen, S., & Savage, C. R., Jr. (1974) *Recent Prog. Horm. Res. 30*, 551–572.
Cohen, S., & Taylor, J. M. (1974) in *Symposium of the Society of Developmental Biology, 30th* (Hay, E. D., King, T. J., & Papaconstantinou, J., Eds.) pp 25–42, Academic Press, New York.
Cohen, S., & Carpenter, G. (1975) *Proc. Natl. Acad. Sci. U.S.A. 72*, 1317–1321.
Cohen, S., Carpenter, G., & Lembach, K. J. (1975) *Adv. Metab. Disord. 8*, 265–284.
De Marco, A., Menegatti, E., & Guarneri, M. (1983) *FEBS Lett. 159*, 201–206.
Dubs, A., Wagner, G., & Wüthrich, K. (1979) *Biochim. Biophys. Acta 577*, 177–194.
Eigen, M. (1964) *Angew. Chem., Int. Ed. Engl. 3*, 1–19.
Englander, S. W., Downer, N. W., & Teitelbaum, H. (1972) *Annu. Rev. Biochem. 41*, 903–924.
Englander, S. W., Calhoun, D. B., Englander, J. J., Kallenbach, N. R., Liem, R. K. H., Malin, E. L., Mandal, C., & Rogero, J. R. (1980) *Biophys. J. 32*, 577–589.
Gregory, H. (1975) *Nature (London) 257*, 325–327.
Gregory, H., & Preston, B. M. (1977) *Int. J. Peptide Protein Res. 9*, 107–118.
Holladay, L. A., Savage, C. R., Cohen, S., & Puett, D. (1976) *Biochemistry 15*, 2624–2633.
Hollenberg, M. D., & Cuatrecasas, P. (1973) *Proc. Natl. Acad. Sci. U.S.A. 70*, 2964–2968.
Hollenberg, M. D., & Cuatrecasas, P. (1975) *J. Biol. Chem. 250*, 3845–3853.
Hollenberg, M. D., & Gregory, H. (1977) *Life Sci. 20*, 267–274.
Jeener, J. (1971) *Magnetic Resonance in Chemistry and Biology, Based on Lectures at the Ampere International Summer School on Magnetic Resonance in Chemistry and Biology*, Basko Polje, Yugoslavia, Marcel Dekker, New York.
Kalinichenko, P. (1976) *Stud. Biophys. 58*, 235–240.
Knox, D. G., & Rosenberg, A. (1980) *Biopolymers 19*, 1049–1068.
Mayo, K. H. (1984) *Biochemistry 23*, 3960–3973.
McDonald, C. C., & Phillips, W. D. (1973) *Biochemistry 12*, 3170–3186.
McKanna, J. A., Haigler, H. T., & Cohen, S. (1979) *Proc. Natl. Acad. Sci. U.S.A. 76*, 5689–5693.
Nagayama, K., & Wüthrich, K. (1981) *Eur. J. Biochem. 114*, 365–374.
Noggle, J. H., & Shirmer, R. E. (1971) *The Nuclear Overhauser Effect*, Academic Press, New York.
O'Keefe, E., Hollenberg, M. D., & Cuatrecasas, P. (1974) *Arch. Biochem. Biophys. 164*, 518–526.
Poulsen, F. M., Hoch, J. C., & Dobson, C. M. (1980) *Biochemistry 19*, 2597–2601.
Pullen, R. A., Lindsay, D. G., Wood, S. P., Tickle, I. J., Blundell, T. L., Wollmer, A., Krail, G., Brandenburg, D., Zahn, H., Gliemann, J., & Gammeltoft, S. (1976) *Nature (London) 259*, 369–373.
Rosa, J. J., & Richards, F. M. (1979) *J. Mol. Biol. 133*, 399–416.
Rosa, J. J., & Richards, F. M. (1981) *J. Mol. Biol. 145*, 835–851.
Savage, C. R., Jr., & Cohen, S. (1972) *J. Biol. Chem. 247*, 7609–7611.
Savage, C. R., Jr., & Cohen, S. (1973) *Exp. Eye. Res. 15*, 361–366.
Savage, C. R., Jr., Inagami, T., & Cohen, S. (1972) *J. Biol. Chem. 247*, 7612–7621.
Savage, C. R., Jr., Hash, J. H., & Cohen, S. (1973) *J. Biol. Chem. 248*, 7669–7672.
Taylor, J. M., Mitchell, W. M., & Cohen, S. (1972) *J. Biol. Chem. 247*, 5928–5934.
Turkington, R. W. (1969) *Exp. Cell. Res. 57*, 79–85.
Wagner, G., & Wüthrich, K. (1979) *J. Magn. Reson. 33*, 675–687.
Wagner, G., Kumar, A., & Wüthrich, K. (1981) *Eur. J. Biochem. 114*, 375–384.
Wüthrich, K., & Wagner, G. (1979) *J. Mol. Biol. 130*, 1–18.
Wüthrich, K., Eugster, A., & Wagner, G. (1980) *J. Mol. Biol. 144*, 601–604.
Wüthrich, K., Wider, G., Wagner, G., & Braun, W. (1982) *J. Mol. Biol. 152*, 311–320.